Far-infrared absorption by interstitial oxygen impurities in silicon crystals

H. Yamada-Kaneta
ULSI Development Division, Fujitsu Limited, 4-1-1 Kamikodanaka, Nakahara-ku, Kawasaki 211-8588, Japan
(Received 14 January 1998)

To verify our model for the local-mode-coupled low-energy excitation of the oxygen in silicon [H. Yamada-Kaneta, C. Kaneta, and T. Ogawa, Phys. Rev. B **42**, 9650 (1990)], we have performed high-resolution far-infrared absorption measurements for the oxygen lines at 29.3, 37.7, 43.3, and 48.6 cm^{-1}. The assignment of these lines to the optical transitions previously made with our model has been supported by the measured temperature dependences of the line intensities. Our model that had explained the line energies has further described successfully the temperature dependence of the line-intensity ratio. This line-intensity ratio is shown to be a manifestation of the quartic anharmonicity (off-center nature) of the potential for the low-energy excitation. [S0163-1829(98)08535-X]

I. INTRODUCTION

The ⟨111⟩ bond-interstitial oxygen in silicon, the Si-O-Si center, causes the far-infrared (FIR) absorption lines at 29.3, 37.7, 43.3, and 48.6 cm^{-1}.[1–3] We refer to these as the 30-cm^{-1} band. It also causes the band in the 1100-cm^{-1} region comprising the lines at 1 136.4, 1 128.2 and 1 121.9 cm^{-1},[1–7] and the band in the 1200-cm^{-1} region having the lines at 1 205.7[1–5,8,9] and 1 216.4 cm^{-1}.[3,8,9] The 30-cm^{-1} band is caused by the two-dimensional (2D) low-energy anharmonic excitation (LEAE) of the oxygen moving in the ⟨111⟩ plane.[2,10] The 1100-cm^{-1} band is due to the A_{2u} local mode in which the oxygen vibrates along the ⟨111⟩ direction.[10] The anharmonic coupling between the 2D LEAE and the A_{2u} local mode causes the 1200-cm^{-1} band as the combination band.[10]

By adjusting the parameters[10] in our model for the A_{2u}-mode-coupled 2D LEAE, we successfully obtained the energy levels and the line assignment [Fig. 4(a) in Ref. 10] that explained the above-mentioned line energies and the temperature dependence of the line intensities[2,4–9] of the 1100- and 1200-cm^{-1} bands. The similar energy-level scheme and the line assignment (Fig. 9 in Ref. 2) had already been suggested by Bosomworth *et al.* However, there has been no experimental check on whether the assignment of the 37.7-, 43.3- and 48.6-cm^{-1} lines in this energy level scheme[2,10] is consistent with the temperature dependences of the intensities of these lines.

Furthermore, we have to demonstrate that our eigenfunctions[3,10] belonging to the adjusted parameter values (Table II in Ref. 3 or Table II in Ref. 10) (Ref. 11) can describe the line intensities as well as the line energies. For the intensity ratio of the 1 205.7-cm^{-1} line to the 1 136.4-cm^{-1} line, our calculated value 0.043 was in good agreement with the measured value 0.038.[3] However, the most fundamental check of the model using the 30-cm^{-1} band remains to be done. There have been no available experimental data on the line-intensity ratio for this band. The resolution of 0.2 cm^{-1} adopted by Bosomworth *et al.*[2] for the first observation to our knowledge, of the 30-cm^{-1} band was insufficient to accurately measure the line intensities at low temperatures.

In this work, we measure temperature dependences of the line intensities in the 30-cm^{-1} band. From this we first confirm the previous line assignments, and next derive the experimental values for the oscillator strength (OS) of the transition for each absorption line. Using our eigenfunctions of the 2D LEAE, we calculate the OS of each transition to compare it with the experimental value. We give a physical interpretation to the obtained OS ratio, referring to the case of the 2D harmonic oscillator (HO).

II. FAR-INFRARED MEASUREMENT

As seen in the next section, the peak height of the 29.3-cm^{-1} line strongly depends on the temperature. Accordingly, to accurately measure the temperature dependence of this line, we need to adopt the sample of appropriate oxygen concentration ($[O_i]$) and sample thickness depending on the temperature. We used six samples listed in Table I to cover the range 7–67 K. They were all grown by the conventional or magnetic-field-imposed Czochralski method. The measuring temperatures for each sample are also given in Table I. For measurement of the temperature dependences of the lines at 37.7, 43.3, and 48.6 cm^{-1}, use of only one sample, MCZ40, was sufficient to cover the temperatures up to 67 K.

TABLE I. The thickness and the relative $[O_i]$ of the samples used for the present FIR measurements. The $[O_i]$ of the MCZ40 sample is 34.3 ppm (Sec. II). The last column shows the measuring temperatures for the 29.3-cm^{-1} line. The substitutional carbon concentrations were less than 0.1 ppm for all samples. They were all *p* type with specific resistivities 8–11 Ω cm.

Sample name	Sample thickness (mm)	$[O_i]$ (Relative value)	Measuring temperatures (K)
MCZ3	7.70	0.117	7, 12
MCZ7	10.00	0.223	15, 19
MCZ15	7.70	0.534	22, 27
84–1	10.10	0.787	32
T1	9.90	0.989	37
MCZ40	20.00	1	32, 37, 42, 47, 52, 57, 62, 67

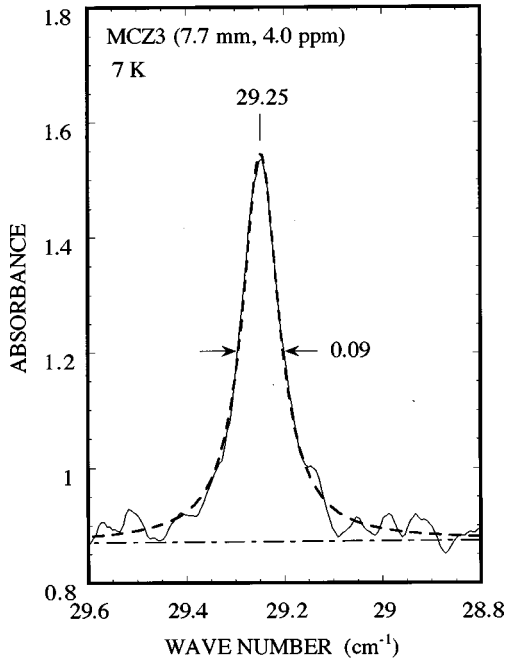

FIG. 1. The 29.3-cm^{-1} line of the MCZ3 sample measured at 7 K with a resolution of 0.01 cm^{-1} (thin solid line). The figure also shows the Lorentz curve (thick dotted line) and its base line (dashed line) fitted to the spectrum in the range 28.8–29.6 cm^{-1}. The values of the line wave number and the FWHM are also shown.

For samples with relatively high $[O_i]$, e.g., 84-1, T1, and MCZ40, the conventional room-temperature infrared-absorption method using the 1106-cm^{-1} line fails to determine the $[O_i]$, because of over range of this absorption. Thus, we employed the 1205.7-cm^{-1} line of oxygen. Table I shows the ratio of the $[O_i]$ of each sample to that of the MCZ40 sample determined by the peak height of this line measured at 7 K and the sample thickness. Using the 1106-cm^{-1} line and the conversion constant given in the American Standard for Testing and Materials F121-79, we determined the $[O_i]$ of the 2-mm-thick specimens cut out from the MCZ40 sample. Averaging these $[O_i]$ values, we found the $[O_i]$ of the MCZ40 sample to be 34.3 ppm.

The FIR absorption spectra were obtained with a BRUKER IFS-120HR Fourier transform spectrophotometer. Measurements for the 29.3-cm^{-1} line were performed with the resolutions 0.01, 0.03, and 0.06 cm^{-1} for temperature ranges 7–22, 27–42, and 47–67 K, respectively. Measurements for the lines at 37.7, 43.3, and 48.6 cm^{-1} were performed with the resolutions 0.03 and 0.06 cm^{-1} for temperature ranges 12–42 and 47–67 K, respectively. The detector was a silicon bolometer. The sample was cooled in a heat-conduction-type cryostat equipped with polyethylene windows. The sample temperature was measured with an accuracy better than 1 K, by a thermocouple attached to the sample holder.

III. RESULT OF MEASUREMENT

Figure 1 shows the 29.3-cm^{-1} line in the absorbance[12] spectrum of the MCZ3 sample measured at 7 K. We see that the shape of this line is Lorentzian. This was the case for all measuring temperatures in this study. The full width at half maximum (FWHM) of this line was 0.09 cm^{-1} at 7 K, which is much narrower than the resolution-limited width 0.2 cm^{-1} reported by Bosomworth *et al.*[2] The FWHM and normalized peak area of the 29.3-cm^{-1} line are plotted in Figs. 2 and 3, respectively, as the functions of the temperature. Here, the normalized peak area means the peak area per sample thickness of 10 mm and $[O_i]$ of 34.3 ppm, i.e., the $[O_i]$ of the MCZ 40 sample. From Fig. 2, we see that our measuring

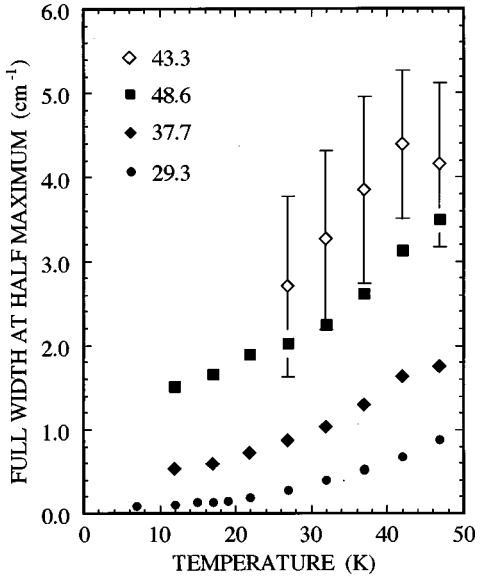

FIG. 2. Observed temperature dependence of the FWHM of the 29.3-, 37.7-, 43.3-, and 48.6-cm^{-1} lines. The top and bottom ends of the error bars correspond to the values obtained by the curve fitting methods (1) and (2), respectively. For the plots without the error bar, the difference in value between the two methods is comparable to or smaller than the size of the plotting marks.

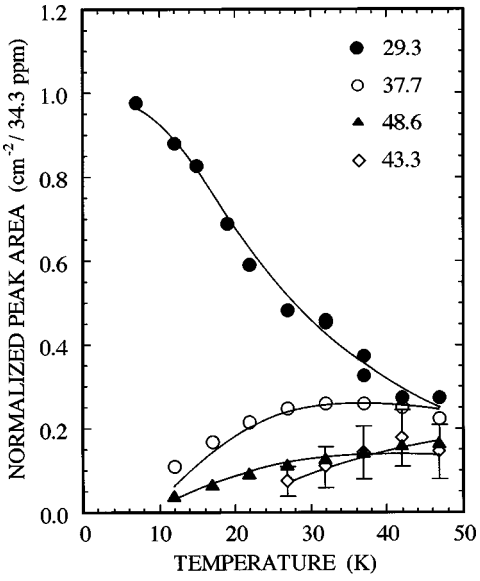

FIG. 3. Temperature dependence of the normalized peak area of the 29.3-, 37.7-, 43.3-, and 48.6-cm^{-1} lines in the absorbance spectrum. The error bars have the same meaning as in Fig. 2. The meaning of the plots without the error bar is also the same. The figure also shows the curves of Eq. (3) drawn with the experimental values of the OS (Table II).

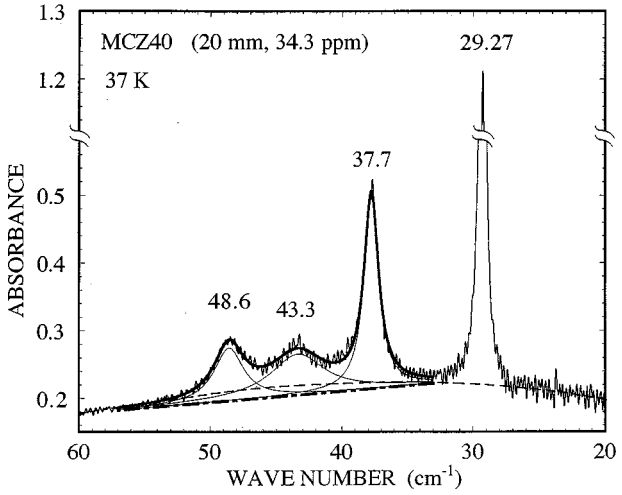

FIG. 4. The 30-cm^{-1} band of the MCZ40 sample measured at 37 K with a resolution of 0.03 cm^{-1}. The figure also shows an example of the curve fitting method (1), where three Lorentz curves (solid curves) and their common base line (dashed line) were fitted to the spectrum in the range 33–57 cm^{-1}. The total fitting curve (thick solid curve) is also shown. The true base line guessed (dotted curve) is slightly protuberant, which was mainly due to insufficiency of stability of the detector, and was inevitable for our high-resolution measurements of long-time data acquisitions. The values of the line wave numbers are also shown.

resolutions for this line (Sec. II) were sufficient to accurately determine its shape and intensity. Figures 2 and 3 indicate that the peak height of the 29.3-cm^{-1} line exhibited very strong temperature dependence: The peak height was reduced to nearly $\frac{1}{34}$ when the temperature was raised from 7 to 47 K.

Figure 4 is the overall spectrum of the MCZ40 sample measured at 37 K. We could not exactly determine the base line for the lines at 37.7, 43.3, and 48.6 cm^{-1}, because of their overlap for a wide range and the protuberance of the base line (dotted curve in Fig. 4). We thus tried the following two manners of curve fitting: (1) As shown in Fig. 4, three Lorentz curves and a linear base line common to them are simultaneously fitted to the spectrum in the range 33–57 cm^{-1}. (2) The fitting range in method (1) is divided into the two ranges 33–41 cm^{-1} and 41–57 cm^{-1}, and the similar curve fittings are performed independently for these two ranges. For both methods (1) and (2), the three peaks were nicely fitted by the Lorentz curves. The FWHM and peak area of these lines were determined by averaging the values obtained by these two methods. Temperature dependences of the FWHM and normalized peak area of these lines are shown in Figs. 2 and 3, respectively. Although the 43.3-cm^{-1} line was observable at 17 and 22 K, it was too weak for accurate curve fitting. This is why the plots for this line are absent for 17 and 22 K in Figs. 2 and 3. From Fig. 2 we see that our measuring resolutions for these lines (Sec. II) were sufficient for accurate measurement.

From Fig. 3, we see that the 43.3-cm^{-1} line is frozen out at nearly 15 K. (At 12 K this line could no longer be observed.) However, the 37.7- and 48.6-cm^{-1} lines both remain until nearly 8 K. This supports the previous line assignments[2,10] where the 37.7- and 48.6-cm^{-1} lines were both ascribed to the transitions from the first excited state and the 43.3-cm^{-1} line was to the transition from the second excited state. These assignments are summarized in Table II.

IV. OSCILLATOR STRENGTH

The eigenstate of the A_{2u}-mode-coupled 2D LEAE is specified by the phonon number N of the A_{2u} local mode, the $\langle 111\rangle$-axial angular momentum l, and the radial quantum number k of the 2D LEAE, i.e., $|k,l,N\rangle$, where N, $k=0,1,2,\ldots$, and $l=0,\pm 1,\pm 2,\ldots$.[3,10] The corresponding eigenfunction is written as[3,10]

$$\Psi_{kl,N}=\xi_{k|l|,N}(r)\,\frac{e^{il\phi}}{\sqrt{2\pi}}\,|N\rangle. \tag{1}$$

(r,ϕ) is the position of the oxygen in the $\langle 111\rangle$ plane. The radial part $\xi_{k|l|,N}(r)$ is obtained numerically as a linear combination of the radial eigenfunctions of a 2D HO.[10] The electric dipole interaction[10] for the optical transition is written as

$$e^{*}r(E_x\cos\,\phi+E_y\sin\,\phi), \tag{2}$$

when the external electric field $\boldsymbol{E}$ is in the $\langle 111\rangle$ plane. For $n=1,2,3\ldots$, two states $|k,n,N\rangle$ and $|k,-n,N\rangle$ degenerate each other, which we express together as $|k,\pm n,N\rangle$. In the transition by Eq. (2), the l changes by ± 1. Therefore, Eq. (2) causes a pair of transitions between the two energy levels of the states $|k,\pm n,0\rangle$ and $|k',\pm(n+1),0\rangle$, for example, $|k,+n,0\rangle\rightarrow|k',+(n+1),0\rangle$ and $|k,-n,0\rangle\rightarrow|k',-(n+1),0\rangle$.

TABLE II. Comparison of the experimental and the theoretical values for the relative OS. The relative OS means the ratio of the OS of each transition to that of the transition $|0,0,0\rangle\rightarrow|0,\pm 1,0\rangle$. The two curve-fitting methods (1) and (2) resulted in the different experimental values for the OS. Their mean value and deviations from it are shown in the third column. The last column shows the relative OS of the corresponding transition in the 2D HO, in which the states $|0,\pm 2,0\rangle$ and $|1,0,0\rangle$ degenerate each other.

Absorption line (cm^{-1})	Assigned transition[a]	Relative OS		
		Experimental	Theoretical	2D HO
29.3	$\|0,0,0\rangle\rightarrow\|0,\pm 1,0\rangle$	1	1	1
37.7	$\|0,\pm 1,0\rangle\rightarrow\|0,\pm 2,0\rangle$	1.60 ± 0.10	1.60	2
48.6	$\|0,\pm 1,0\rangle\rightarrow\ \|1,0,0\rangle$	0.61 ± 0.03	0.60	1
43.3	$\|0,\pm 2,0\rangle\rightarrow\|0,\pm 3,0\rangle$	2.88 ± 1.30	2.08	3

[a]References 2 and 10.

TABLE III. The moment of inertia of the probability density distribution $\int_0^\infty dr\ r^3|\xi_{kl,0}(r)|^2$ calculated for each eigenstate of the present 2D LEAE and the 2D HO. The values shown are the ratio of the calculated value for each state to that for the ground state $|0,0,0\rangle$.

Eigenstate $\lvert k,l,0\rangle$	Moment of inertia of the probability density distribution	
	2D LEAE	2D HO
$\lvert 0,0,0\rangle$	1	1
$\lvert 0,\pm 1,0\rangle$	1.59	2
$\lvert 1,0,0\rangle$	1.80	3
$\lvert 0,\pm 2,0\rangle$	2.08	3

Every absorption line in the 30-cm^{-1} band is caused by this type of the paired transitions (Table II).

From Eqs. (1) and (2), the area of the absorption line by the transition between $|k,\pm n,0\rangle$ and $|k',\pm(n+1),0\rangle$ is expressed as

$$c(\rho_{kn,0}-\rho_{k'n+1,0})(E_{k'n+1,0}-E_{kn,0}) \times\left(\int_0^\infty dr\ r^2\xi_{k'n+1,0}(r)\xi_{kn,0}(r)\right)^2, \qquad (3)$$

where c is a const, $\rho_{kn,0}$ is the Boltzmann occupation probability for the state $|k,n,0\rangle$, and $E_{kn,0}$ is its eigenenergy. By the factor $[\int_0^\infty dr\ r^2\xi_{k'n+1,0}(r)\xi_{kn,0}(r)]^2$ in Eq. (3), we define the OS of the transition between $|k,\pm n,0\rangle$ and $|k',\pm(n+1),0\rangle$. The eigenenergies can be obtained by applying our energy-level diagram (Fig. 3 of Ref. 10) to the previously fixed parameter values (Table II in Ref. 3). The eigenenergies of several low lying states have been shown in Fig. 2 of Ref. 13. Substituting these values of $E_{kn,0}$ into Eq. (3), and regarding the OS as the adjustable parameter, we fitted Eq. (3) to the plots in Fig. 3. The result is shown in the figure by the solid curves. The relative values for the adjusted OS are given in Table II as the experimental values. By using the eigenfunctions (1) belonging to the previously fixed parameter values (Table II in Ref. 3), we numerically calculated the OS. The relative values for the calculated OS are given in Table II as the theoretical values. They are in excellent agreement with the experimental values, confirming validity of our model[10] of the A_{2u}-mode-coupled 2D LEAE.

Table II also compares the OS ratio of the present 2D LEAE, 1:1.6:0.6:2.08, with that of the 2D HO, 1:2:1:3. For the present 2D LEAE, the OS of the transition from the ground state $|0,0,0\rangle\rightarrow|0,\pm 1,0\rangle$ is not so small, as compared with those of the transitions from the excited states. For example, the ratio of the OS of this transition to that of $|0,\pm 1,0\rangle\rightarrow|0,\pm 2,0\rangle$ is 1/1.6, which is larger than the corresponding ratio 1/2 in the 2D HO. This is a manifestation of an important aspect of the present 2D LEAE: the off-center nature (quartic anharmonicity) (Ref. 10) of the potential for the 2D LEAE. The off-center nature widens the bottom of the potential to give large spread to the ground-state wave function. To quantify the spread of the wave function, we adopt the moment of inertia of the probability density distribution, $\int_0^\infty dr\ r^3|\xi_{kn,0}(r)|^2$. Table III lists the relative values of this quantity calculated for each eigenstate of the present 2D LEAE and the 2D HO.[14] For the present 2D LEAE, the spread of the ground state is so large that the ratio of this spread to that of the first excited state takes a large value of 1/1.59. This is in contrast to the small value 1/2 for the corresponding ratio in the 2D HO. Consequently, for the present 2D LEAE, the transition from the ground state has a relatively large OS.

To summarize, high-resolution FIR absorption measurements have been carried out for the lines at 29.3, 37.7, 43.3, and 48.6 cm^{-1} of the Si-O-Si center. An experimental confirmation has been given to the previous assignment[2,10] of these lines to the optical transitions. This further confirms the energy-level scheme[2,10] itself in which these transitions were defined. The oscillator strength ratio of the optical transitions derived from the measurement has well agreed with that calculated with our model[10] that explained the line energies previously. It has been shown that this oscillator strength ratio is a manifestation of the quartic anharmonicity (off-center nature) of the potential for the low-energy excitation.

ACKNOWLEDGMENTS

The author is indebted to Dr. Y. Furumura and T. Yabu of Fujitsu Ltd. for their constant encouragement for basic research.

[1] The wave numbers of the absorption lines appearing in this paper are those determined in this study or in our latest measurements. Some of these wave numbers are slightly different from those reported before.

[2] D. R. Bosomworth, W. Hayes, A. R. L. Spray, and G. D. Watkins, Proc. R. Soc. London, Ser. A **317**, 133 (1970).

[3] H. Yamada-Kaneta, C. Kaneta, and T. Ogawa, Phys. Rev. B **47**, 9338 (1993).

[4] H. J. Hrostowski and R. H. Kaiser, Phys. Rev. **107**, 966 (1957).

[5] H. J. Hrostowski and B. J. Alder, J. Chem. Phys. **33**, 980 (1960).

[6] B. Pajot, J. Phys. Chem. Solids **28**, 73 (1967).

[7] K. Krishnan and S. L. Hill, in *Fourier Transform Infrared Spectroscopy*, edited by H. Sakai (SPIE, Bellingham, WA, 1981), p. 221.

[8] B. Pajot, H. J. Stein, B. Cales, and C. Naud, J. Electrochem. Soc. **132**, 3034 (1985).

[9] B. Pajot and B. Cales, in *Oxygen, Carbon, Hydrogen and Nitrogen in Crystalline Silicon*, MRS Symp. Proc. No. 59, edited by

J. C. Mikkelsen, Jr., S. J. Pearton, J. W. Corbett, and S. J. Pennycook (Materials Research Society, Pittsburgh, 1986), p. 39.

[10] H. Yamada-Kaneta, C. Kaneta, and T. Ogawa, Phys. Rev. B **42**, 9650 (1990).

[11] In Ref. 10, our model parameters had been fitted to the line energies reported in Refs. 2, 4–6, 8, and 9. In Ref. 3, for consistency and precision, we again fitted the parameters to our measured line energies. These two sets of parameter values, almost equal to each other, cause no innegligible difference in the calculational results.

[12] Here, the absorbance is defined by $-\log_{10}[I(\omega)/I_0(\omega)]$.

[13] H. Yamada-Kaneta, C. Kaneta, and T. Ogawa, Mater. Sci. Forum **83-87**, 419 (1992).

[14] For the 2D HO, the OS of the transition $|0,\pm n,0\rangle \rightarrow |0,\pm(n+1),0\rangle$ is equal to the moment of inertia of the probability density distribution of the initial state, i.e., $[\int_0^\infty dr\ r^2 \xi_{0n+1,0}(r)\xi_{0n,0}(r)]^2 = \int_0^\infty dr\ r^3 |\xi_{0n,0}(r)|^2$. The present numerical calculation suggests that also for the present 2D LEAE, this relation approximately holds for small n (see Tables II and III).